

**Xanthorrhizol-induced apoptosis  
signaling pathway in oral squamous  
carcinoma cells**

**Kim Ju Yeon**  
**Department of Medical Science**  
**The Graduate School, Yonsei University**

**Xanthorrhizol-induced apoptosis  
signaling pathway in oral squamous  
carcinoma cells**

Kim Ju Yeon

Department of Medical Science

The Graduate School, Yonsei University

Xanthorrhizol-induced apoptosis  
signaling pathway in oral squamous  
carcinoma cells

Directed by Professor Seo Jeong Taeg

The Master's Thesis  
submitted to the Department of Medical Science,  
the Graduate School of Yonsei University  
in partial fulfillment of the requirements for the degree of  
Master of Medical Science

Kim Ju Yeon

December, 2004

This certifies that the Master's Thesis  
of Kim Ju Yeon is approved.

---

Seo Jeong Taeg

---

Kim Hye Young

---

Chung Won Yoon

The Graduate School  
Yonsei University

December, 2004

# Acknowledgements

I would like to send great thanks in my heart to my kind supervisor Jeong Taeg Seo for guiding me friendly to finish the graduate course well.

I really appreciate Professor Kim Hye Young and Professor Chung Won Yoon having made time for advising my dissertation.

It's my great pleasure to thank Professor Syng Ill Lee, Professor Dong Min Shin, Professor Yun Jung Yoo, Professor Jeong Heon Cha, and Professor Sang Hwuy Lee.

It's my luck to have been with the members of the pharmacological part during Master's course. I am very pleased with expressing thanks to the members. Especially thanks to Research fellow Jeong Mi Ahn giving me a careful concern, Soo Young having been with me all the time, Hye Eun assisting me, and Hyo Sook being a member of our part a few months ago. From the heart, I want to tell Du Sik to be my fiancés that I thank for everything.

I am very grateful to every member of the department of Oral Biology, who made me encouraged. Thank Hyun Ju, Hae Mi, Min Seok, Cho Hae, Seong Hye, Teaching assistant Jeong Hee Hong, Soo Hyun, Nam Ho, Hye Jin, Tae Jin, Heui Jung, Postdoc Jae Young Kim, Kyoung won, Jong Min, Jinglei Cai, Research fellow Sung Won Cho, Sun Young, Woo Cho and Jeong Ah.

Finally, special thanks go to my family for always making me to cheer up and supporting. And thank my old friends very much for being great help besides me.

## Table of contents

Abstract .....	1
I. INTRODUCTION .....	3
II. MATERIALS AND METHODS .....	9
1. Materials .....	9
2. Methods .....	9
A. Cell culture .....	10
B. Fluorescence-activated cell sorter (FACS) analysis .....	10
C. MTT assay .....	10
D. Western blot analysis .....	11
E. Measurement of intracellular $\text{Ca}^{2+}$ concentration ( $[\text{Ca}^{2+}]_i$ ) .....	11
F. Hoechst 33258-propidium iodide counterstaining .....	12
G. Statistical analysis .....	12
III. RESULTS .....	13
1. Xanthorrhizol induced cell death in a dose-dependent manner. .....	13
2. Xanthorrhizol was shown to induce early and late apoptosis depending on the increase of the concentration. ....	13
3. PARP cleavage was implicated in xanthorrhizol-induced cell death, but the cleavage pattern of PARP was not typical. ....	17
4. Xanthorrhizol-induced cell death was mediated by caspase- independent pathway. ....	19
5. Xanthorrhizol led to an increase in $[\text{Ca}^{2+}]_i$ .....	19

6. Xanthorrhizol-induced cell death was not attributed to $[Ca^{2+}]_i$ increase .....	22
7. Xanthorrhizol activated MAP kinases in a time-dependent manner. ....	22
8. Inhibition of p38 and JNK prevented cell death caused by xanthorrhizol. ....	25
IV. DISCUSSION .....	28
V. CONCLUSION .....	32
REFERENCES .....	33

## List of figures

Figure 1. Xanthorrhizol induced cell death in SCC-15 cells. ....	14
Figure 2. Annexin V-positive cells increased depending on the concentration of xanthorrhizol. ....	15
Figure 3. Xanthorrhizol-treated cells were shown to have morphological characteristics of early apoptosis and late apoptosis. ....	16
Figure 4. Full length PARP, caspase-3 substrate, was cleaved by xanthorrhizol treatment in a dose-dependent manner, but not in a typical manner. ....	18
Figure 5. Z-VAD-fmk, a pan-caspase inhibitor, did not prevent xanthorrhizol-activated signaling pathway. ....	20
Figure 6. Caspase-3 was not activated by xanthorrhizol. ....	21
Figure 7. Intracellular $Ca^{2+}$ was elevated by xanthorrhizol treatment. ....	23
Figure 8. EGTA/AM, intracellular $Ca^{2+}$ chelator, had no preventive effect on xanthorrhizol-induced cell death. ....	24
Figure 9. Xanthorrhizol activated MAP kinases in a time-dependent manner. ....	26
Figure 10. SAPK inhibitors contributed to inhibiting xanthorrhizol-induced cell death. ....	27

Abstract

# Xanthorrhizol-induced apoptosis signaling pathway in oral squamous carcinoma cells

Kim Ju Yeon

*Department of Medial Science*

*The Graduate School, Yonsei University*

(Directed by Professor Seo Jeong Taeg)

In this study, xanthorrhizol, a natural compound isolated from *Curcuma xanthorrhiza roxb*, was shown to have an anti-carcinogenic effect and induce apoptosis in SCC-15 cells. Xanthorrhizol was found to induce cell death of SCC-15 cells in a dose-dependent manner ( $EC_{50} = 47.7 \mu\text{M}$ ). Flow cytometry analysis and Hoechst 33258 and PI double staining revealed that SCC-15 cells underwent early apoptosis and late apoptosis depending on the concentration of xanthorrhizol and the time. In addition, cells treated with xanthorrhizol showed cleavage of the

full-length poly [ADP (ribose)] polymerase (PARP; 118 KDa), but full length PARP was not typically cleaved into an 85 KDa fragment in response to xanthorrhizol. Caspase-3 was not activated and pretreatment with Z-Val-Ala-Asp-fluoromethylketone (Z-VAD-fmk), a pan-caspase inhibitor, could not rescue apoptotic cells. However, xanthorrhizol was shown to exert time-dependent activation of ERK, JNK, and p38 in SCC-15 cells. The activation of ERK, JNK, and p38 were observed 6-12 hr after xanthorrhizol treatment. To examine the role of MAPKs in xanthorrhizol-induced apoptosis, the cells were pretreated with the inhibitors of ERK, JNK and p38 such as PD98059, SP600125 and SB203580, respectively. SP600125 and SB203580 reduced xanthorrhizol-induced apoptosis, whereas PD98059 did not prevent the xanthorrhizol-induced apoptosis. Combined treatment with SP600125 and SB203580 had an additive effect. In conclusion, the results indicated that xanthorrhizol caused the activation of ERK, JNK and p38, but ERK contributed little to the signaling pathway leading to apoptosis in SCC-15 cells while JNK and p38 appeared to play a critical role in xanthorrhizol-induced apoptosis.

---

Key words : SCC-15 cells, xanthorrhizol, PARP, caspases, MAPKs

# Xanthorrhizol-induced apoptosis signaling pathway in oral squamous carcinoma cells

Kim Ju Yeon

*Department of Medical Science*

*The Graduate School, Yonsei University*

(Directed by Professor Seo Jeong Taeg)

## I. Introduction

Apoptosis is an intrinsic death program that plays a crucial role in the regulation of cellular homeostasis. Breaking out of a balance between cell death and proliferation by the external stress leads to the tumor formation. And also, tumor cells are killed by chemical and physical means predominantly mediated through apoptosis. Therefore, how well tumor cells can evade engagement of apoptosis shows how resistant to cancer treatments tumor cells are. In developing effective treatments

against cancer cells, it is important to understand that an anticancer drug targets signals connected with apoptosis, and then passes through a series of apoptotic events, resulting in apoptosis of tumor cells.

Curcuma is a member of the Zingiberaceae/Ginger family, which consists of *C. longa*, *C. xanthorrhiza*, *C. aromatica*, and *C. zedoaria*. Among these members, curcumin isolated from *c. longa* has been commonly known as a drug to exert anti-hepatotoxic, anti-inflammatory, anti-oxidative, anti-carcinogenic, and anti-microbial effects. It has been reported that *C. xanthorrhiza* also has anti-inflammatory<sup>1</sup>, anti-tumor<sup>2</sup>, and hepatoprotective activities<sup>3</sup>. Xanthorrhizol derived from *C. xanthorrhiza* already has been reported to possess the contractile activity of uterine smooth muscle<sup>4</sup> and a potential antibacterial effect against *Streptococcus mutants*<sup>5</sup>. And also, recently, xanthorrhizol was shown to have a protective effect against cisplatin-induced hepatotoxicity<sup>6</sup>. However, it has not been known yet whether xanthorrhizol, a natural compound isolated from *C. xanthorrhiza* which has been reported to possess an antitumor effect, has this effect.

The major characteristics of apoptosis include appearance of phosphatidylserine (PS) on the external cell membrane, loss of mitochondrial transmembrane potential, the activation of the caspase family, cleavage of the poly [ADP-(ribose)] polymerase (PARP), nuclear chromatin condensation, and DNA

fragmentation<sup>7</sup>. The typical signaling pathway leading to apoptosis is known as receptor-mediated and chemical-induced apoptosis<sup>8,9</sup>. Generally, most cytokines, the member of tumor necrosis factor (TNF) family, induce apoptosis through binding the ligand to its death receptor. Fas-associated death domain (FADD) is serially docking to TNF receptor, and then activates FADD-like interleukin-1 converting enzyme (FLICE) and caspase-3, which is a group of cystein proteases and takes a role in cleavage of various substrates such as PARP resulting in apoptosis. In contrast, chemicals (most chemotherapeutic agents)-induced apoptosis is involved in cleavage of BID by activation of caspase-8, which leads to release cytochrome c from the mitochondria, and then cytochrome c together with the apoptotic protease activity factor-1 (APAF-1) induces activation of caspase-9. After that, PARP cleavage is induced by activation of caspase-3. It has been known that the chemical-induced apoptotic pathway including mitochondria is negatively regulated by inhibiting cytochrome c release through the interaction of antiapoptotic protein such as Bcl-2 or Bcl-xl<sup>10,11,12</sup>.

Proteins comprising the mitogen-activated protein kinase (MAPK) family constitute important mediators of signal transduction processes that take a role in responding to the external stress. The MAPK superfamily is made up of three main signaling pathways; the extracellular signal-regulated protein kinases (ERKs), the c-Jun N-terminal kinases or stress-

activated protein kinases (JNK/SAPK), and the p38 family of kinases. The MAPK, known as a serine/threonine kinase, is activated by a MAPK kinase (MAPKK), which has a dual phosphorylation site involving both Ser/Thr and Tyr, targeting a Thr-X-Tyr motif on the MAPK (where X is glutamate, proline or glycine for the ERK, JNK and p38 modules, respectively)<sup>13</sup>. The MAPK signaling cascades control cell growth, differentiation and death by phosphorylating various target proteins, many of which are nuclear proteins such as transcription factors. The ERK module has been known as signaling cascades related to cell proliferation, development, differentiation, and cellular survival. The stimuli such as growth factors activate c-Raf, which sequentially allows ERK1/2 phosphorylated by MAPK/ERK kinase (MEK)1 and MEK2 to be activated<sup>14</sup>. Upon translocation to the nucleus, ERKs are responsible for the phosphorylation of multiple substrates, depending on the initial stimulus. In contrast, JNK and p38 are generally shown to respond to a variety of cytokines and stress including tumor necrosis factor, ionizing and short wave length ultraviolet irradiation (UVC), and hyperosmotic stress<sup>15-19</sup>. The JNKs are activated by dual phosphorylation at the Thr-Pro-Tyr motif by JNKK1 and JNKK2, also known as MAPK kinase 4 (MKK4) and MKK7<sup>20</sup>. Activation of the JNK signaling cascade is generally associated with apoptosis, inflammation, and tumorigenesis. Also, the p38 MAPK module has dual phosphorylation site at Thr-Gly-Tyr motif and

involves MKKs 3 and 6 as upstream kinases acting on p38. It is known that p38 controls cell motility, apoptosis, chromatin remodeling, and osmoregulation<sup>21</sup>. In the various recent studies, it is suggested that MAPK cascades mediate cellular death signaling processes responding to various anticarcinogenic agents. In Caov-3 and A2780 ovarian carcinoma cell line, cisplatin, an anticancer drug, was reported to induce a rapid activation of ERK<sup>12,22</sup>. Also, in Hela cell (human cervical carcinoma cell), PD98059, MEK inhibitor, prevented cell death induced by cisplatin, which was suggested that MEK inhibitor interfered cytochrome c release, activation of caspase-3, and PARP cleavage<sup>23</sup>. KB3 cell line which stably expressed c-Jun dominant negative deletion mutant exhibited that not only phosphorylation of c-Jun, activating transcription factor-2, and AP-1 activation were strongly inhibited, but also caspase-3 activation was delayed when vinblastine, an important anticarcinogen inducing G<sub>2</sub>-M arrest, was treated<sup>24</sup>. In Hela cells, four chemotherapeutic agents were shown to induce p38 activation and mitotic cell cycle arrest by depolymerizing (nocodazole, vincristine, and vinblastine) or stabilizing (taxol) microtubules<sup>25</sup>.

Calcium is an intracellular messenger in a cellular signaling process. The function of Ca<sup>2+</sup> in apoptosis is related to many cellular systems, the sphingomyelin signaling pathway, the redox system, the stress-activated protein kinase cascade and the

Ca<sup>2+</sup> signaling pathway. Ca<sup>2+</sup> regulates pro-apoptotic (Bax, Bak, and Bad) and anti-apoptotic (Bcl-2 and Bcl-X<sub>L</sub>) proteins<sup>26</sup>. It was reported that exposure to the synthetic triterpenoid 2-cyano-3,12-dioxooleana1,9-dien-28-oic acid (CDDO), a novel anti-cancer agent, led to the disruption of intracellular Ca<sup>2+</sup> homeostasis associated with the cell death, and intracellular calcium chelator inhibited caspase activation induced by CDDO<sup>27</sup>.

Using the squamous carcinoma cell line, I investigated if xanthorrhizol is able to act as a pharmacologically safe anticancer agent and through which pathway xanthorrhizol induces apoptosis.

## II. Materials and Methods

### 1. Materials

DMEM/F-12(1:1) media, Fetal Bovine Serum (FBS), antibiotics and trypsin-EDTA(1X) were from GIBCO (Grand Island, NY, USA). Hydrocortisone and MTT were obtained from Sigma-aldrich (St. Louis, MO, USA). Annexin-V-FLUOUS Staining Kit was from Roche (Manheim, Germany), and Z-Val-Ala-Asp-fluoromethylketone (Z-VAD-fmk), PD98059, SB203580 and SP600125 were purchased from Calbiochem (La Jolla, CA, USA). Anti-ERK, anti-phospho-ERK, anti-JNK, anti-phospho-JNK, anti-p38, anti-phospho-p38 and anti-PARP antibodies were obtained from Cell signaling technology (Beverly, MA, USA). Fura-2/AM, Pluronic F-127, and Hoechst 33258 were purchased from Molecular probes (Eugene, OR, USA).

### 2. Methods

#### A. Cell culture

Squamous carcinoma cell-15 (SCC-15) line was obtained from American Type Culture Collection (ATCC, Manassas, VA, USA). The cells were maintained in DMEM/F-12 (1:1) media containing 10% fetal bovine serum, 1% antibiotics, and 400 ng/ml hydrocortison at 37 °C in a humidified atmosphere of 5 % CO<sub>2</sub> and 95 % air. The medium was changed every 2 days and the subculture was performed every 7 days using 0.25 % trypsin and

1 mM EDTA solution.

#### B. Fluorescence-activated cell sorter (FACS) analysis

$1 \times 10^6$  cells were plated in 60 mm culture plate and treated with xanthorizol in the indicated concentration. After induction of apoptosis, the cells were trypsinized, washed with ice-cold phosphate buffered saline (PBS) twice. Subsequently, cells were resuspended and incubated in the dark condition with 100  $\mu$ l of double staining agent, which includes fluorescein isothiocyanate (FITC) conjugated annexin V and propidium iodide (PI) for 10 min at room temperature. Stained cells were analyzed by Flow Cytometry (BD Calibur, Beckman Coulter).

#### C. MTT assay

Approximately  $8 \times 10^4$  cells/well were plated in 24-well plates. After each indicated treatment, 50  $\mu$ l stock 3-(4,5-dimethylthiazol-2-yl)-2,5-diphenyl-tetrazolium bromide (MTT, 5mg/ml in sterile phosphate-buffered saline) was added and incubated for 2 hr at 37 °C. Finally, 300  $\mu$ l of solubilizing solution (50 % dimethylformamide and 20% sodium dodecyl sulfate, pH 4.8) was added. After an overnight incubation at 37 °C, the optical densities at 570 nm were measured using a 96-well multiscanner autoreader (Dynatech MR 5000), with the extraction buffer as a blank. Cell viability was determined as % relative cell viability =  $[(\text{experimental-blank})/(\text{control-blank})] \times 100$ , where experimental and control were the values for the treated cells and untreated cells, respectively.

#### D. Western blot analysis

For immunoblot analysis, cells were collected, and then washed out with phosphate-buffered saline (PBS) twice. Collected cells were allowed to incubate for 1hr on ice in 50 $\mu$ l of lysis buffer (50 mM Tris-Cl (pH 7.4), 150 mM NaCl, 1 % TritonX-100, 100  $\mu$ g/ml phenylsulfonyl fluoride (PMSF), 1  $\mu$ g/ml aprotinin, 1 mM dithiothreitol (DTT), 1 mM Na<sub>3</sub>VO<sub>4</sub>). The resulting cell lysates were resolved on 8-12 % SDS-PAGE and transferred onto nitrocellulose membrane (Protran, Bioscience). The membranes were blocked with Tris-buffered saline with 5 % skim milk in tween 20 [10 mM Tris-Cl (pH 7.5), 150 mM NaCl, 0.1 % Tween 20] and then hybridized with different antibodies. Proteins were detected by using luminol chemiluminescent substrate (LumiGLO, Cell Signaling Technology).

#### E. Measurement of intracellular Ca<sup>2+</sup> concentration ([Ca<sup>2+</sup>]<sub>i</sub>)

Cells were loaded with fura 2 by incubation with 2  $\mu$ M fura 2-acetoxymethyl ester in HEPES-buffered solution equilibrated with 100% O<sub>2</sub> for 40 min at room temperature. They were washed twice and resuspended in an HCO<sub>3</sub><sup>-</sup>-buffered solution containing (in mM) 110 NaCl, 4.5 KCl, 1.0 NaH<sub>2</sub>PO<sub>4</sub>, 1.0 MgSO<sub>4</sub>, 1.5 CaCl<sub>2</sub>, 25 NaHCO<sub>3</sub>, 5 HEPES-Na, 5 HEPES free acid, and 10 D-glucose and equilibrated with 95% O<sub>2</sub>-5% CO<sub>2</sub> to give pH 7.4. The cells were allowed to attach to a coverslip, which formed the base of a cell chamber mounted on the stage of an inverted

microscope. Once the cells had adhered to the coverslip, they were continuously superfused with the  $\text{HCO}_3^-$ -buffered solution at a flow rate of 2 ml/min. And then, xanthorrhizol (1  $\mu\text{M}$  and 30  $\mu\text{M}$ ) in the  $\text{HCO}_3^-$ -buffered solution was flowed onto the cells. All experiments were carried out at 37°C.  $[\text{Ca}^{2+}]_i$  was measured by spectrofluorometry (Photon Technology International, Brunswick, NJ), with excitation at 340 and 380 nm and emission at 510 nm.

#### F. Hoechst 33258-propidium iodide counterstaining

Cells were trypsinized and collected. Cell pellets ( $1 \times 10^6$ ) were suspended by 100  $\mu\text{l}$  PBS containing Hoechst33258 (10  $\mu\text{M}$ ). The cells were incubated at 37 °C for 7min, and then centrifuged. The cell pellets were resuspended in 100  $\mu\text{l}$  staining solution containing propidium iodide (10  $\mu\text{M}$ ). The stained cells were analyzed using a fluorescence microscope (LEICA/DM LB/Fluorescence).

#### G. Statistical analysis

The statistical significances of differences between the positive- and negative-regulated groups were determined by using a one-way ANOVA and Bonferroni's test. A *P* value <0.05 was considered statistically significant. The results are expressed as means  $\pm$ SD.

### III. Results

#### 1. Xanthorrhizol induced cell death in a dose-dependent manner.

To examine the cytotoxicity of xanthorrhizol, cells were treated with various doses of the drug for 24 hr. After the treatment, the viable cells were measured by MTT assay. Xanthorrhizol caused cell death of SCC-15 cells in a dose-dependent manner. Cell viability was reduced by approximately 40 % of the cell population by the treatment of 20  $\mu\text{M}$  xanthorrhizol for 24 hr. The cell viability was fallen by 60% when cells were treated with 60  $\mu\text{M}$  xanthorrhizol.

#### 2. Xanthorrhizol was shown to induce early and late apoptosis depending on the increase of the concentration.

By FACS analysis using Annexin V and PI double staining, two classical early events of apoptotic cell death, the translocation PS from inner side of the cytoplasm membrane to the outer side and the loss of mitochondrial membrane potential, were observed. In figure 2, the annexin V positive but PI negative cells ( the right lower quadrant) were detected at the concentration of 60  $\mu\text{M}$  xanthorrhizol for 24 hr, and the population of annexin V and PI positive cells (end stage apoptosis and necrotic cell) increased when cells were treated

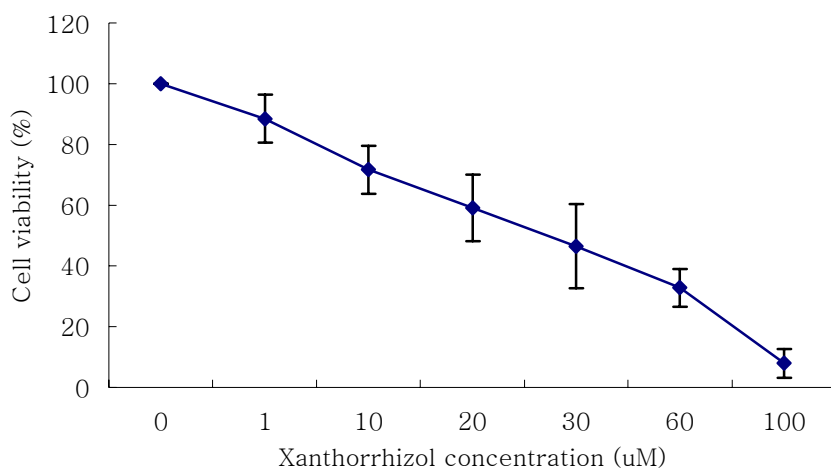
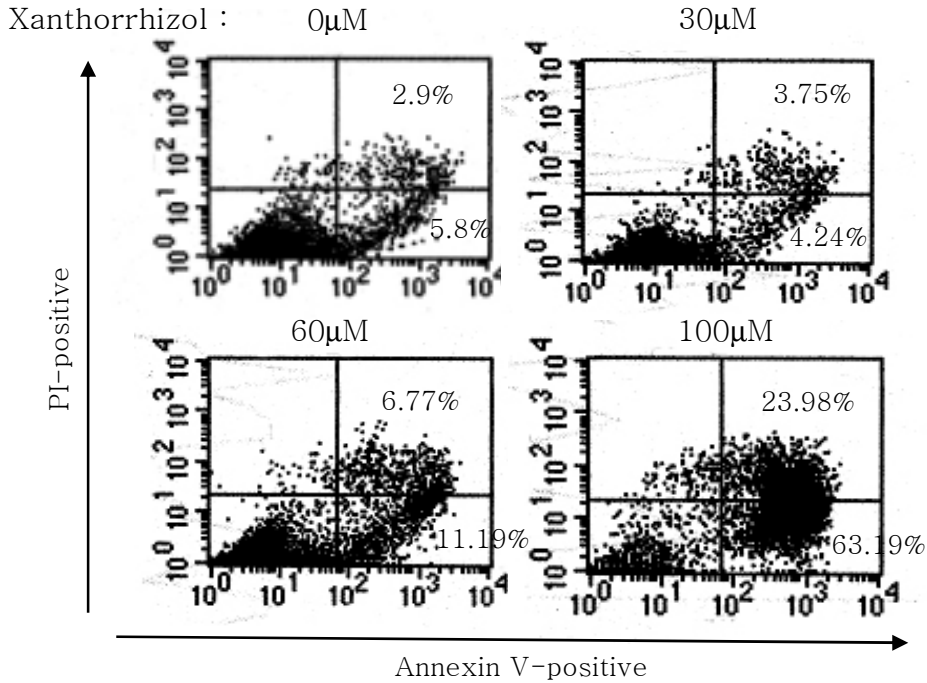


Figure 1. Xanthorrhizol induced cell death in SCC-15 cells. Cells were plated, and then treated with various concentrations of xanthorrhizol for 24 hr. After the incubation, cell viability was determined by MTT assay (n=6).



Necrotic cells	Late apoptotic cells
Viable cells	Early apoptotic cells

Figure 2. Annexin V-positive cells increased depending on the concentration of xanthorrhizol. After treatment of xanthorrhizol for 24 hr, cells were trypsinized and collected, and then stained with annexin V and PI dye. Dot plots of the results revealed viable ( lower left quadrant), early apoptotic (annexin-V-positive; lower right quadrant), late apoptotic (upper right quadrant), and necrotic(PI-positive; upper left quadrant) (n=3).

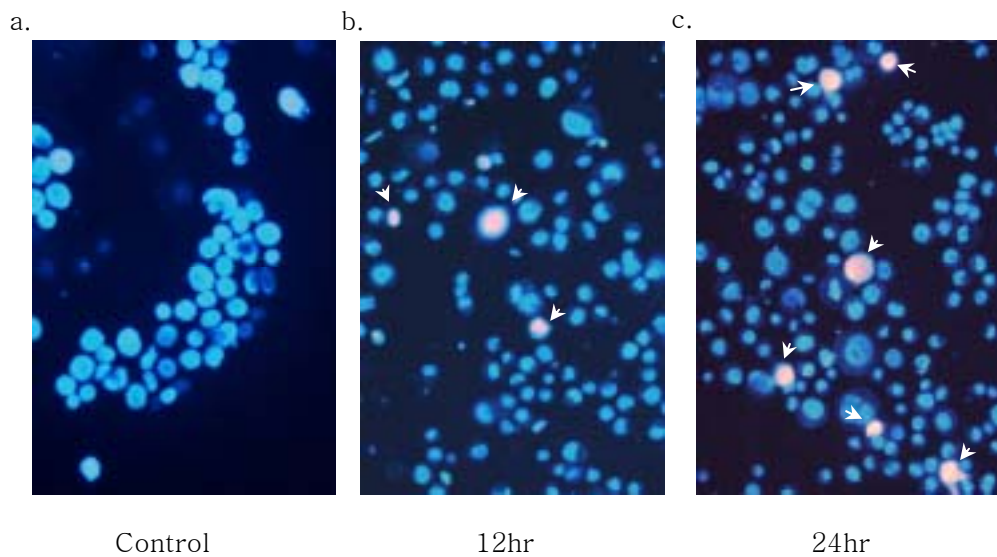


Figure 3. Xanthorrhizol-treated cells were shown to have morphological characteristics of early apoptosis and late apoptosis. Cells were treated with or without 60  $\mu\text{M}$  xanthorrhizol for 12hr or 24hr. And then cells were stained with Hoechst 33258 (10  $\mu\text{M}$ ) and propium iodide (10  $\mu\text{M}$ ), and examined by fluorescence microscopy. Round blue nuclei revealed viable cells, fragmented blue nuclei revealed early apoptotic cells, and round pink nuclei revealed late apoptotic cells (white arrow head).

with the concentration of 100  $\mu\text{M}$  xanthorrhizol. The population of the early apoptotic cells increased from 5% to 11 % by the treatment of 60  $\mu\text{M}$  xanthorrhizol and increased further into 63.19 % by 100  $\mu\text{M}$  xanthorrhizol with simultaneous increase of the late apoptotic cells. And also, I examined the morphological characteristics of xanthorrhizol-induced cell death using fluorescence microscopy after double staining with Hoechst 33258 and propidium iodide (PI). In figure 3, viable cells showed round blue nuclei stained with Hoechst 33258, late apoptotic cells showed round pink nuclei stained with both Hoechst 33258 and PI, and early apoptotic cells showed fragmented blue nuclei. Without xanthorrhizol, most cells showed round blue nuclei (figure 3a), but treated with 60  $\mu\text{M}$  xanthorrhizol, nuclei-fragmented cells increased in a time-dependent manner (figure 3b). And cells having round pink nuclei slightly increased over time (figure 3c).

3. PARP cleavage was implicated in xanthorrhizol-induced cell death, but the cleavage pattern of PARP was not typical.

To examine the activation of cellular caspase induced by xanthorrhizol, PARP cleavage was detected by Western blot analysis. Cells were treated with various concentrations of xanthorrhizol for 24 hr. After exposure to xanthorrhizol, cell lysates (40  $\mu\text{g}$ ) were subjected to 8 % SDS PAGE, and

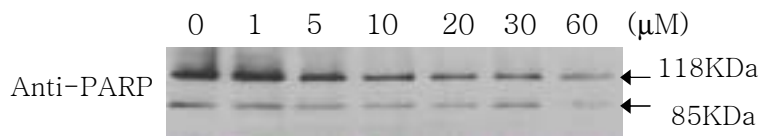


Figure 4. Full length PARP, caspase-3 substrate, was cleaved by xanthorrhizol treatment in a dose-dependent manner, but not in a typical manner. Cells were incubated with the indicated concentrations of xanthorrhizol for 24 hr. After cells were harvested and lysated, 40  $\mu\text{g}$  of cell lysates was subjected to SDS-PAGE, and PARP cleavage was detected with an anti-PARP antibody as described under materials and methods (n=3).

then probed with anti-PARP antibody (1:1500). Full length PARP of 118 KDa was cleaved by xanthorrhizol in a dose-dependent manner, however it was not split into the cleaved PARP of 85 KDa. As exposure to higher concentration of xanthorrhizol, both full-length PARP and 85 KDa cleaved PARP decreased simultaneously. PARP seemed to be cleaved into much smaller fragments, but it was failed to detect them in this study.

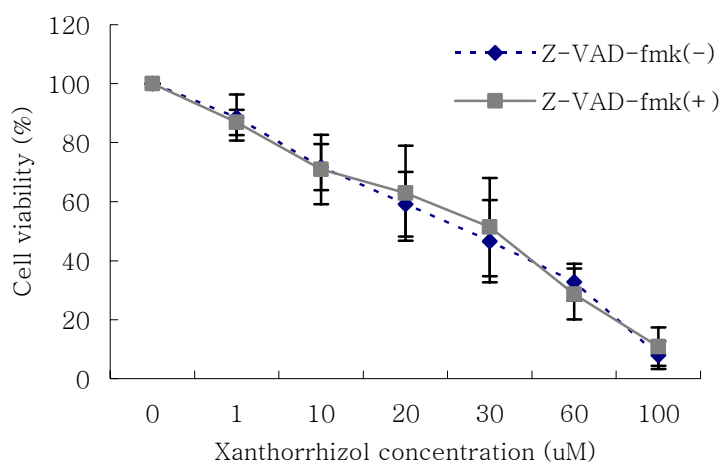
4. Xanthorrhizol-induced cell death was mediated by caspase-independent pathway.

To investigate the involvement of caspases in xanthorrhizol-induced cell death, cell viability and PARP cleavage were measured using Z-VAD-fmk, a pan-caspase inhibitor and examined the activation of caspase-3 through Western blot analysis. The concentration of 50  $\mu$ M Z-VAD-fmk was pretreated for 1 hr before xanthorrhizol was added. As shown in figure 5, Z-VAD-fmk pretreatment did not prevent cell death and PARP cleavage. In figure 6, the activation of caspase-3 also was not observed.

5. Xanthorrhizol led to an increase in  $[Ca^{2+}]_i$ .

To test the effect of intracellular  $Ca^{2+}$  on xanthorrhizol-induced apoptosis, the change of  $[Ca^{2+}]_i$  was measured using fura-2

A.



B.

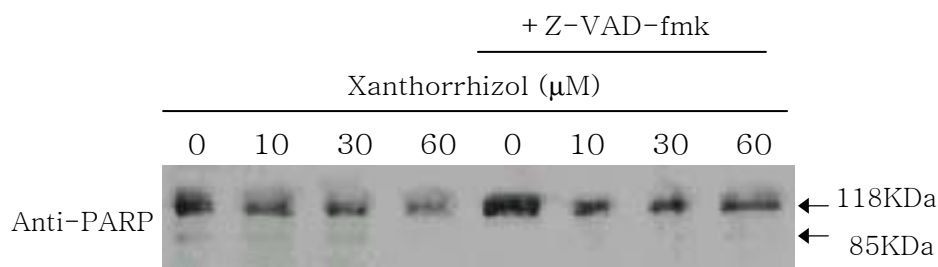


Figure 5. Z-VAD-fmk, a pancaspase inhibitor, did not prevent xanthorrhizol-induced cell death. A. Z-VAD-fmk, could not rescue cells from death induced by xanthorrhizol (n=5). B. Z-VAD-fmk did not prevent PARP cleavage in SCC-15 cells (n=3). The concentration of 50  $\mu$ M Z-VAD-fmk was pretreated for 1hr before the treatment of xanthorrhizol and cells were further incubated with various concentrations of xanthorrhizol for 24hr. Cell viability was determined by MTT assay, and PARP cleavage was detected by Western blot analysis as described in materials and methods.

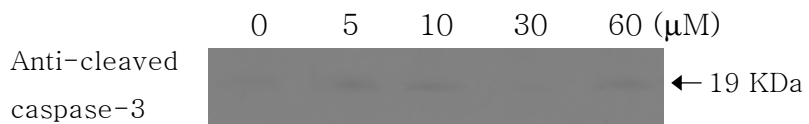


Figure 6. Caspase-3 was not activated by xanthorrhizol. Cells were treated with the indicated concentrations for 24hr. After cells were harvested and lysated, 60  $\mu\text{g}$  of cell lysates was subjected to SDS-PAGE, and the activation of caspase-3 was detected using cleaved caspase-3 antibody to detect the activated caspase-3 (n=4).

fluorescence technique. Buffer solution containing 1  $\mu\text{M}$  or 30  $\mu\text{M}$  xanthorrhizol was perfused and  $[\text{Ca}^{2+}]_i$  was found to increase by 30  $\mu\text{M}$  xanthorrhizol.

6. Xanthorrhizol-induced cell death was not attributed to  $[\text{Ca}^{2+}]_i$  increase.

To investigate the relationship between the increase in  $[\text{Ca}^{2+}]_i$  and the cell death induced by xanthorrhizol, cells were treated with xanthorrhizol in the presence or absence of EGTA/AM, an intracellular  $\text{Ca}^{2+}$  chelator. Cells were pretreated with 2  $\mu\text{M}$  EGTA/AM for 1 hr and then incubated with xanthorrhizol for additional 24 hr. Pretreatment with EGTA/AM did not prevent the cell death induced by xanthorrhizol, shown as figure 8.

7. Xanthorrhizol activated MAP kinases in a time-dependent manner.

To investigate the other possible mechanism of xanthorrhizol-induced cell death, the effect of xanthorrhizol on MAPK activation was examined. Cell lysates obtained at the indicated times from xanthorrhizol-treated cells were subjected to Western blot analysis using anti-phospho ERK, JNK, and p38 antibodies to detect phosphorylated ERK, JNK and p38. The same blots were subsequently stripped and reprobed with

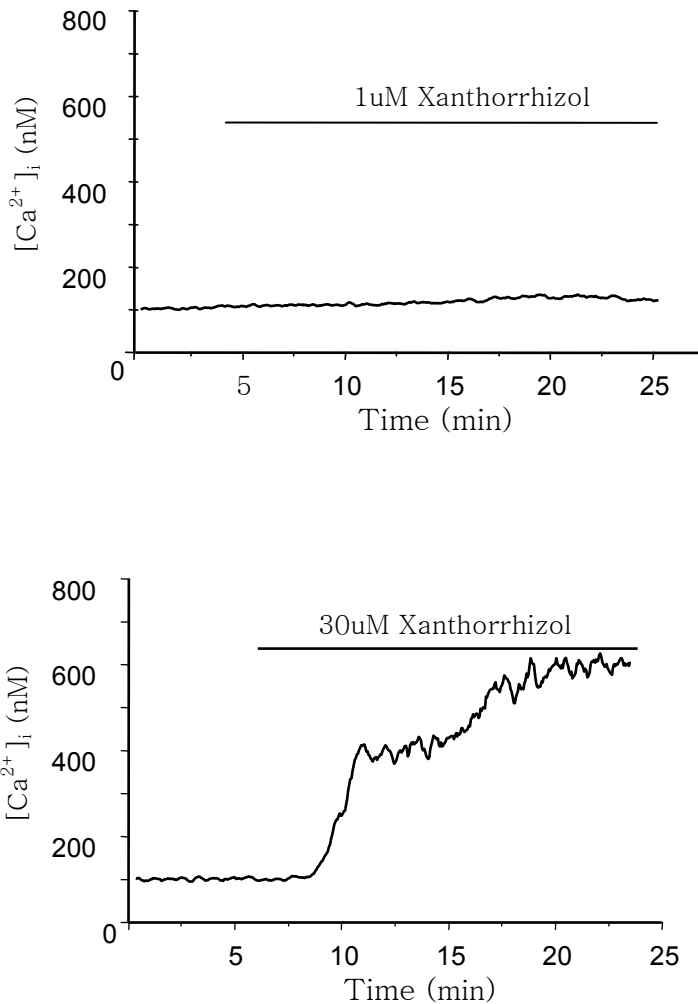


Figure 7. Intracellular  $Ca^{2+}$  was elevated by xanthorrhizol treatment. The cells were plated on 24x24 mm cover glasses 2 days before the experiment, and loaded with fura-2/AM for 30 min. The physiological solution containing 1mM  $Ca^{2+}$  was allowed to flow on the cover glass for 5 min, and then the buffer including the indicated concentration of xanthorrhizol was perfused for further 20 min (n=3)

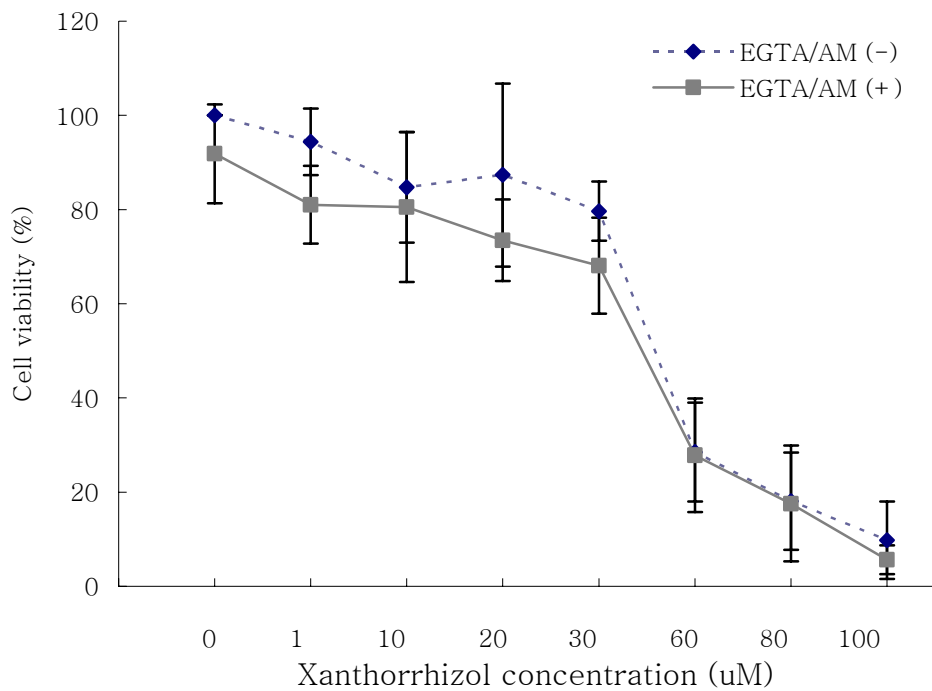


Figure 8. EGTA/AM, an intracellular  $\text{Ca}^{2+}$  chelator, had no preventive effect on xanthorrhizol-induced cell death. Cells were pretreated with (—■—) or without (---◆---) 2  $\mu\text{M}$  EGTA/AM for 1 hr followed by treatment with various concentrations of xanthorrhizol. Cell viability was determined by MTT assay (n=3).

antibodies that recognize total ERK, JNK, and p38 to verify equal amounts of the protein in the various samples. As shown in the figure 7, treatment with 60  $\mu$ M xanthorrhizol led to an activation of ERK time dependently, reaching maximum at 12 h. And also, both JNK and p38, stress-activated kinases, were monitored in response to xanthorrhizol in various time courses. p38 activation occurred over the same time period as ERK, whereas JNK activation occurred slightly prior to activations of ERK and p38.

#### 8. Inhibition of p38 and JNK prevented cell death caused by xanthorrhizol.

SCC-15 cells were exposed to 60  $\mu$ M xanthorrhizol for 24 hr in the presence of MAP kinase inhibitors such as PD98059 (50  $\mu$ M), SB203580 (20  $\mu$ M), and SP600125 (40  $\mu$ M), which inhibited phospho-ERK, phospho-p38, and phospho-JNK, respectively. Each inhibitor of MAP kinases was pretreated for 1 hr prior to the treatment of 60  $\mu$ M xanthorrhizol. PD98059 could not efficiently rescue xanthorrhizol-induced cell death; however SB203580 attenuated the cell death by 20 %, and SP600125 had a more efficient effect on rescuing the cells exposed to xanthorrhizol. In addition, combined-treatment with SB203580 and SP600125 was shown to have the most efficient effect on the increase of cell viability from 40 % to 70 %.

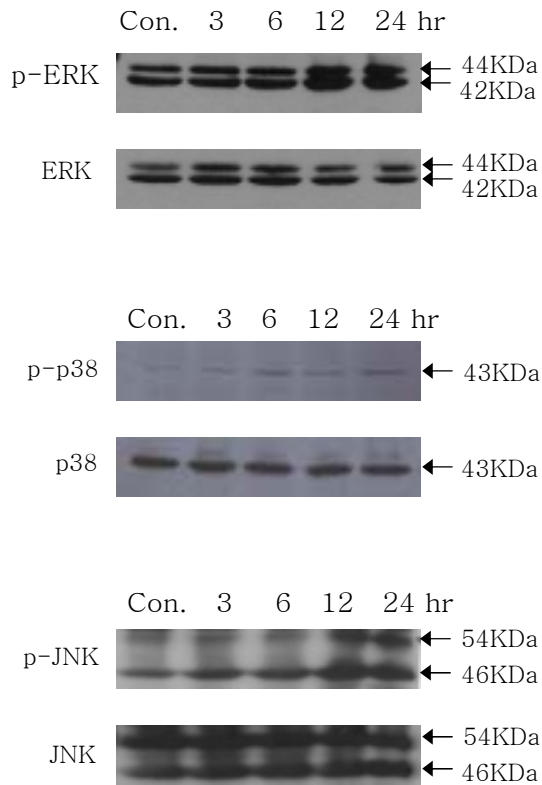


Figure 9. Xanthorrhizol activated MAP kinases in a time-dependent manner. Cells were seeded in 60 mm culture dishes 2 days before the experiment was performed. The concentration of 60  $\mu$ M xanthorrhizol was treated for the indicated times. After the incubation, cell lysates (40  $\mu$ g) were subjected to SDS-PAGE gel and immunoblotted with anti-phospho ERK, anti-ERK, anti-phospho p38, anti-p38, anti-phospho JNK, and anti-JNK antibodies.

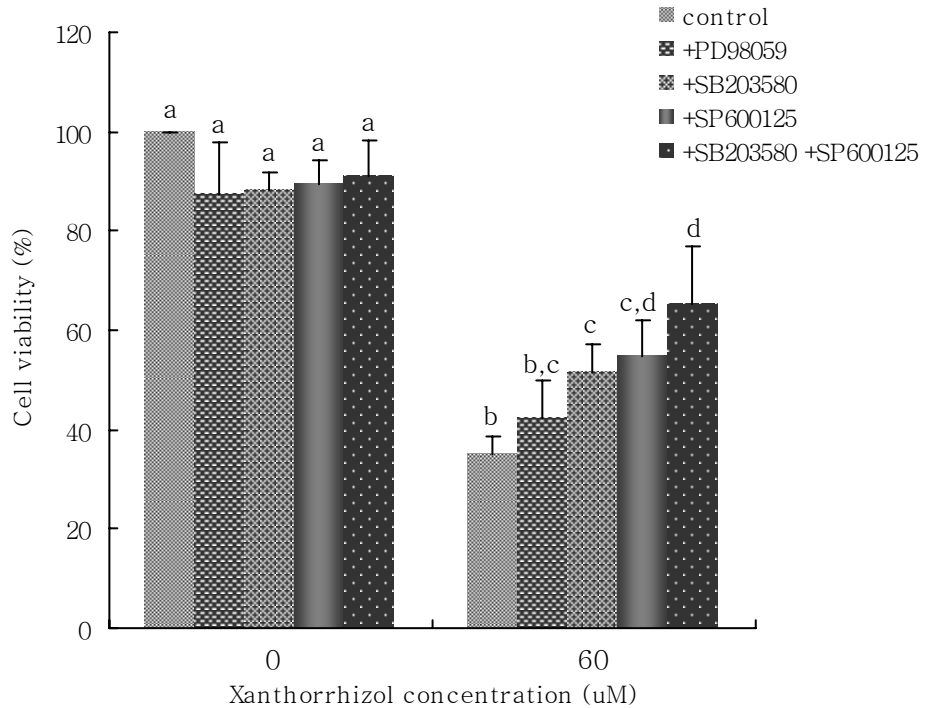


Figure 10. SAPK inhibitors prevented xanthorrhizol-induced cell death. Both SB203580 and SP600125, which inhibited p-p38 and p-JNK respectively, were shown to suppress xanthorrhizol-induced cell death but PD98059, a MEK inhibitor, failed to rescue cell death induced by xanthorrhizol. All MAP kinase inhibitors, PD98059 (50  $\mu$ M), SB203580 (20  $\mu$ M), and SP600125 (40  $\mu$ M), were pretreated for 1hr and then the cells were incubated in the presence or absence of xanthorrhizol (60  $\mu$ M) for 24 hr (n=4). Values are means  $\pm$ SD. Means with different lowercase letters are significantly different at  $P < 0.05$ .

#### IV. Discussion

Apoptosis is mediated by various cellular events including protein synthesis and degradation, the alteration in protein phosphorylation states, the activation of the second messenger systems such as  $\text{Ca}^{2+}$ , and disruption of normal mitochondrial function. In this study, I found that xanthorrhizol might play an effective role as the anti-cancer drug in SCC-15 cells and activate a regulatable suicide program, which is distinct from the classic caspase-dependent apoptotic cell death. In HL-60 cells, during ectoposide-induced apoptosis PARP was cleaved into typical fragments of 89KDa and 24KDa, whereas cytochalasin B cleaved PARP into major fragments of 89 KDa and 50 KDa and minor fragments of 40 KDa and 35 KDa, which were not the typical size to be observed when general apoptotic process occurred<sup>28</sup>. In the present study, for the process of apoptosis induced by xanthorrhizol, PARP, the nucleus protein, was atypically cleaved; full-length PARP was cleaved, but 85 KDa cleaved PARP also was further fragmented into cleaved PARP of smaller size than that of 85 KDa size. But, cleaved PARP of smaller size could not be identified in SCC-15 cells. In addition, Z-VAD-fmk failed to prevent xanthorrhizol-induced cell death as well as PARP cleavage, and the activation of caspase-3 also was not detected. These results suggested that xanthorrhizol did not activate caspase-dependent signaling, and PARP cleavage

might depend on the other target protein related to apoptosis. According to many reports, change of intracellular  $\text{Ca}^{2+}$  concentration to be served as the second messenger to regulate cellular homeostasis, was correlated not only with pro-apoptotic and anti-apoptotic protein but also with caspase activation. It has been reported that in human colorectal cancer cells, the increase of intracellular  $\text{Ca}^{2+}$  concentration was involved in parthenolide-induced apoptosis<sup>29</sup>. However, although xanthorrhizol caused intracellular  $\text{Ca}^{2+}$  increase, xanthorrhizol-induced cell death was not abrogated by chelating increased intracellular  $\text{Ca}^{2+}$  using EGTA/AM. This result indicated that  $\text{Ca}^{2+}$  did not take a part in xanthorrhizol-induced cell death.

It has been reported by several groups that various anti-cancer drugs such as ceramide, vinblastine, and cisplatin induced apoptosis through MAPK pathway. In Hela cell, ERK activation was involved in the cisplatin-induced apoptosis<sup>23</sup>. In A431 cells, both caspase-dependent and -independent signaling participated in ceramide-induced apoptosis, in which both ERK and p38 of MAPKs were activated. However, the inhibition of ERK activation by MEK inhibitor PD98059 had no effect on rescuing ceramide-induced cell death, whereas the inhibition of p38 MAP kinase by specific inhibitor SB203580 prevented ceramide-induced cell death<sup>30</sup>. It was informed that p38 but not ERK pathway took an important role in ceramide-induced cell death, which is consistent with the results that in SCC-15 cells,

although xanthorrhizol contributed to the activation of both ERK and p38. Based on the present data, xanthorrhizol stimulated all MAP kinases, which sustained to be activated for 24 hr. Actually it has been reported that ERK signaling was mostly related to cell survival, but in the recent study, reactive oxygen species (ROS) caused ERK activation, which induced cytochrome c release, to result in the activation of caspase family<sup>23</sup>. Despite ERK activation, MEK inhibitor (PD98059) was not able to suppress cell death induced by xanthorrhizol. It was thought that ERK signaling might not act as one of the cell death signals, but endeavors of cell survival. It was also reported that in HCT116 human colon cancer cells, curcumin stimulated JNK and p38 pathway, but the specific JNK inhibitor SP600125 solely had an effect on interfering curcumin-induced apoptosis; therefore, curcumin induced in JNK-dependent apoptosis<sup>31</sup>. According to the results, p38 inhibitor (SB203580) was shown to prevent xanthorrhizol-induced cell death. In addition, xanthorrhizol precipitated phosphorylation of JNK and SP600125 offered resistance to xanthorrhizol-induced cell death. Furthermore, the combined treatment with SB203580 and SP600125 enhanced the ability to survive by blocking both p38 and JNK pathway in xanthorrhizol-induced cell death. It was shown that xanthorrhizol led to the cell death through stress-activated kinase (SAPK) pathway. In summary, the present data indicated that in SCC-15 cells, xanthorrhizol-induced apoptosis was

blocked by inhibiting either JNK or p38, or both of them but not caspase. However, in the process of apoptotic events, the atypical cleavage of PARP was observed. The data implicated that SAP kinase signaling was mostly involved in xanthorrhizol-induced apoptosis rather than caspase signaling, and atypical cleavage of PARP might be occurred by the other protease, but not caspase.

## V. Conclusion

1. Xanthorrhizol induced cell death in a dose-dependent manner in SCC-15 cells.
2. Xanthorrhizol-induced cell death was shown to atypical cleavage of PARP.
3. Z-VAD-fmk, pan-caspase inhibitor, could not rescue cell death induced by xanthorrhizol.
4. Xanthorrhizol exerted to activate all MAP kinases, which were consisted of ERK, JNK, and p38, in a time-dependent manner.
5. PD98059, MEK inhibitor, could not prevent xanthorrhizol-induced cell death, whereas SP600125 and SB203580, JNK and p38 inhibitor, were effectively contributed to suppress xanthorrhizol-induced cell death.
6. SAP kinases signaling might play a critical role in xanthorrhizol-induced cell death.

In conclusion, xanthorrhizol induced cell death in SCC-15 cells, which might depend on SAP kinases signaling.

## References

1. Ozaki Y. Antiinflammatory effect of *Curcuma xanthorrhiza* Roxb, and its active principles. *Chem Pharm Bull (Tokyo)*. 1990;38(4):1045-1048
2. Itokawa H, Hirayama F, Funakoshi K, Takeya K. Studies on the antitumor bisabolane sesquiterpenoids isolated from *Curcuma xanthorrhiza*. *Chem Pharm Bull (Tokyo)*. 1985;33(8):3488-3492
3. Lin SC, Lin CC, Lin YH, Supriyatna S, Teng CW. Protective and therapeutic effects of *Curcuma xanthorrhiza* on hepatotoxin-induced liver damage. *Am J Chin Med*. 1995;23(3-4):243-254
4. Ponce-Monter H, Campos MG, Aguilar I, Delgado G. Effect of xanthorrhizol, xanthorrhizol glycoside and trachylobanoic acid isolated from Cachani complex plants upon the contractile activity of uterine smooth muscle. *Phytother Res*. 1999;13(3):202-205
5. Hwang JK, Shim JS, Baek NI, Pyun YR. Xanthorrhizol: a potential antibacterial agent from *Curcuma xanthorrhiza* against *Streptococcus mutans*. *Planta Med*. 2000;66(2):196-197
6. Kim SH, Hong KO, Chung WY, Hwang JK, Park KK. Abrogation

of cisplatin-induced hepatotoxicity in mice by xanthorrhizol is related to its effect on the regulation of gene transcription.

*Toxicol Applied pharmacol.* 2004;196(3);346-355

7. Blatt NB, Glick GD. Signaling pathways and effector mechanisms pre-programmed cell death. *Bioorg Med Chem.* 2001;9(6);1371-1384

8. Ashkenazi A, Dixit VM. Apoptosis control by death and decoy receptor. *Curr.Opin. Cell Biol.* 1999;11;255-260

9. Wang TH, Popp DM, Wang HS, Saitoh M, Mural JG, Henley DC, Ichijo H, Wimalasena J. Microtubule dysfunction induced by paclitaxel initiates apoptosis through both c-Jun N-terminal kinase (JNK)-dependent and-independent pathways in ovarian cancer cells. *J Biol Chem.* 1999;274;8208-8216

10. Meiyun F, Timothy C, Chambers TC. Role of mitogen-activated protein kinases in the response of tumor cells to chemotherapy. *Drug Resistance Updates.* 2001;5;253-267

11. Minn AJ, Swain RE, Ma A. Thompson CB. Recent progress on the regulation of apoptosis by Bcl-2 family members. *Adv. Immunol.* 1998;70;245-279

12. Yang J, Liu X, Bhalla K, Kim CN, Ibrado AM, Cai J, Peng TI, Jones DP, Wang X. Prevention of apoptosis by Bcl-2: release of cytochrome c from mitochondria blocked. *Science* 1997;275(5303); 1129-1132
13. Hoeflich KP, Woodgett JR. Signal transduction and gene expression in the regulation of natural freezing survival. *Cell and molecular responses to stress* 2001;2; 175-193
14. Moodie SA, Wolfman A. The 3Rs of life: Ras, Raf, and growth regulation. *Trends Genet.* 1994;10; 44-48
15. Wang X, Martindale JL, Liu Y, Holbrook NJ. The cellular response to oxidative stress: influences of mitogen-activated protein kinase signaling pathways on cell survival. *Biochem. J.*1998; 333;291-300
16. Xia Z, Dickens M, Raingeaud J, Davis RJ, Greenberg ME. Opposing effects of ERK and JNK-p38 MAP Kinases on apoptosis. *Science* 1995; 270;1326-1331
17. Chen YR, Wang X, Templeton D, Davis RJ, Tan TH. The Role of c-Jun N-terminal Kinase (JNK) in apoptosis induced by ultraviolet C and  $\gamma$  radiation. Duration of JNK activation may determine cell death and proliferation. *J. Biol. Chem.*

1996;271;31929-31936

18. Graves JD, Draves KE, Craxton A, Saklatvala J, Krebs EG, Clark EA. Involvement of stress-activated protein kinase and p38 mitogen-activated protein kinase in mIgM-induced apoptosis of human B lymphocytes. *Proc. Natl. Acad. Sci.* 1996;93;13814-13818

19. Brenner B, Koppenhoefer U, Weinstock C, Linderkamp O, Lang F, Gulbins E. Fas- or Ceramide-induced Apoptosis Is Mediated by a Rac1-regulated Activation of Jun N-terminal Kinase/p38 Kinases and GADD153. *J. Biol. Chem.* 1997;272;22173-22181

20. Tournier C, Whitmarsh AJ, Cavanagh J, Barrett T, Davis RJ. The MKK7 gene encodes a group of c-Jun NH2-terminal kinase kinases. *Mol. Cell. Biol.* 1999;19(2); 1569-1581

21. New L, Han J. The p38 MAP kinase pathway and its biological function. *Trends Cardiovasc.Med.* 1998;8;220-229

22. Hayakawa J, Ohmichi M, Kurachi H, Ikegami H, Kimura A, Matsuoka T, Jikihara H, Mercola D, Murata Y. Inhibition of extracellular signal-regulated protein kinase or c-Jun N-terminal protein kinase cascade, differentially activated by

cisplatin, sensitizes human ovarian cancer cell line. *J. Biol. Chem.* 1999;274,31648–31654

23. Wang X., Martindale JL, Holbrook NJ. Requirement for ERK activation in cisplatin-induced apoptosis. *J. Biol. Chem.* 2000;275(50): 39435–39443

24. Fan M, Goodwin ME, Birrer MJ, Chambers TC. The c-Jun NH(2)-terminal protein kinase/AP-1 pathway is required for efficient apoptosis induced by vinblastine. *Cancer research*, 2001;61(11);4450–4458

25. Olson JM, Hallahan AR. p38 MAP kinase: convergence point in cancer therapy. *TRENDS in Molecular Medicine.* 2004;10(3);125–129

26. Berridge MJ, Lipp P, Bootman MD. The versatility and universality of calcium signaling. *Mol. Cell Biology.* 2000;1;11–21

27. Numsen Hail, Jr., Marina Konopleva, Michael Sporn, Reuben Lotan, and Michael Andreeff . Evidence Supporting a Role for Calcium in Apoptosis Induction by the Synthetic Triterpenoid 2-Cyano-3,12-dioxooleana-1,9-dien-28-oic Acid (CDDO). *J. Biol. Chem.* 2004;279;11179–11187

28. Shah GM, Shah RG, Poirier GG. Different cleavage pattern for poly(ADP-ribose) polymerase during necrosis and apoptosis in HL-60 cells. *Biochem Biophys Res Commun.* 1996; 29:838-844

29. Siyuan Zhang, Choon-Nam Ong and Han-Ming Shen; Critical roles of intracellular thiols and calcium in parthenolide-induced apoptosis in human colorectal cancer cells. *Cancer Letters* 2004; 208:143-153

30. Zhao S, Yang YN, Song JG. Ceramide induces caspase-dependent and -independent apoptosis in A-431 cells. *Journal of cellular physiology.* 2004;199:47-56

31. Collett GP, Campbell FC. Curcumin induces c-jun N-terminal kinase dependent apoptosis in HCT116 human colon cancer cells. *Carcinogenesis* Advance Access published July 15 2004

Abstract (in korean)

## 구강암 세포주에서 xanthorrhizol에 의해 유도된 세포사멸 기전

<지도교수 서정택>

연세대학교 대학원 의과학과

김주연

*Curcuma xanthorrhiza* Roxb로부터 추출한 xanthorrhizol이 구강암 세포주인 SCC-15 세포에서 항암 효과를 가지며 세포 사멸을 유도하는 것을 확인하였다. 본 실험에서, xanthorrhizol에 의한 세포 사멸은 농도 의존적으로 증가하였고( $EC_{50} = 47.7 \mu M$ ) flow cytometry analysis와 Hoechst 33258, propidium iodide (PI) double staining을 통해 xanthorrhizol에 의해 유도된 세포사멸은 사멸이 진행됨에 따라 early apoptosis에서 late apoptosis가 증가하는 것을 보여주었다. 게다가 caspase의 기질인 full-length poly [ADP-(ribose)] polymerase (PARP; 118 KDa)의 절단이 xanthorrhizol 농도의 증가에 따라 일어났지만 PARP의 절단 형태는 전형적인 세포사멸에서 관찰되어지는 형태가 아니었다. 또한 caspase의

억제제인 Z-Val-Ala-Asp-fluoromethylketone (Z-VAD-fmk)를 전처리 하였을 때 xanthor-rhizol로 유도된 세포사멸을 막을 수 없었고 caspase-3 또한 활성화되지 않았다. 그러나 xanthorrhizol은 구강암 세포주에서 mitogen-activated kinases (MAPKs)인 ERK, JNK, 그리고 p38 모두를 6-12시간 사이에 활성화 시켰고 24시간 동안 지속적으로 활성화 되어있었다. Xanthorrhizol에 의해 유도되는 세포사멸 기전에서 MAPKs의 역할을 규명하기 위해 ERK 억제제인 PD98059, JNK 억제제인 SP600125, p38 억제제인 SB203580을 전처리 하였을 때, PD98059는 xanthorrhizol에 의해 유도된 세포사멸을 막지 못하였으나, SP600125와 SB203580은 세포 사멸을 억제 하였다. 또한 SP600125와 SB203580을 함께 전처리 하였을 때 각각을 처리한 군보다 세포 사멸을 더 효과적으로 막을 수 있었다. 결론적으로 xanthorrhizol은 ERK, JNK, 그리고 p38 모두를 활성화 시켰으나 stress-activated kinases인 JNK와 p38이 xanthorrhizol에 의해 유도된 세포사멸 기전에 가장 중요한 역할을 하는 것으로 보인다.

---

핵심되는 말 : SCC-15 cells, xanthorrhizol, PARP, caspases, MAPKs